Hemilabile silver(I) complexes containing pyridyl chalcogenolate (S, Se) ligands and their utility as molecular precursors for silver chalcogenide

Goutam Kumar Kole[a], K. V. Vivekananda[a], Mukesh Kumar[b], Rakesh Ganguly[c], Sandip Dey[a] and Vimal K. Jain[a,*]

[a]Chemistry Division, [b]Solid State Physics Division, Bhabha Atomic Research Centre, Mumbai 400085, India

Email: jainvk@barc.gov.in; Tel: +91 22 2559 5095; Fax: +91 022 2550 5151

[c]Division of Chemical and Biological Sciences, School of Physical and Mathematical Sciences, Nanyang Technological University, Singapore – 637371

Table S1: Parameters for hydrogen bonding and other weak interactions in **1**.

D-H$\cdots$A	D(D-H) (Å)	D(H$\cdots$A) (Å)	D(D$\cdots$A) (Å)	<(DHA) (°)	Symmetry Operator
N(1)-H(1N)$\cdots$N(1)	0.76(6)	1.90(6)	2.656(3)	176(7)	1-x,y,1/2-z
C(16)-H(16) $\cdots$S(1)	0.95(1)	2.91(1)	3.673(6)	138.1(1)	2-x, 1-y, 1-z

Table S2: Parameters for hydrogen bonding in **4**.

D-H$\cdots$A	D(D-H) (Å)	D(H$\cdots$A) (Å)	D(D$\cdots$A) (Å)	<(DHA) (°)	Symmetry Operator
O(2)-H(2A)$\cdots$N(2)	0.85	2.08	2.86(2)	151.72	-
O(2)-H(2B)$\cdots$O(1)	0.85	2.08	2.59(3)	118.16	-

Table S3: Parameters for hydrogen bonding in **5**.

D-H$\cdots$A	D(D-H) (Å)	D(H$\cdots$A) (Å)	D(D$\cdots$A) (Å)	<(DHA) (°)	Symmetry Operator
O(1)-H(1)$\cdots$O(2)	0.82	1.94	2.755(16)	175.81	2-x,1-y,1-z
O(2)-H(2A)$\cdots$N1	0.82	1.95	2.749(14)	164.8	1+x, y, z
C(47)-H(47)$\cdots$O(1)	0.93	2.39	3.268(16)	156.25	2-x, -y, 1-z

Table S4: Parameters for hydrogen bonding and weak interactions in **6**.

D-H···A	D(D-H) (Å)	D(H···A) (Å)	D(D···A) (Å)	<(DHA) (°)	Symmetry Operator
O(60)-H(60)···N1	0.82	2.20	2.98(2)	158.61	-
C(19)-H(19)···S1 (intramolecular)	0.93	2.75	3.57(12)	147.96	-
C(33)-H(33)···S1	0.93	2.96(6)	3.84(6)	158.54	-
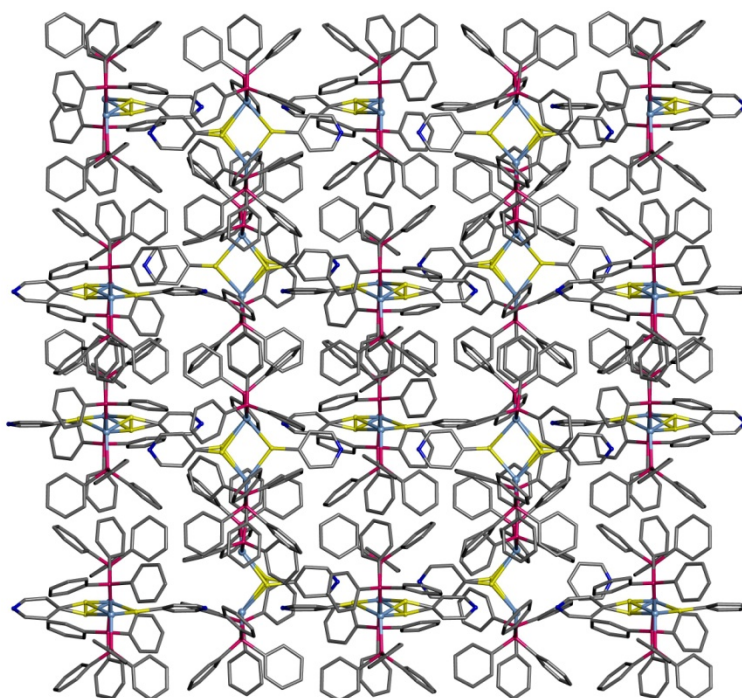
Figure S1: Packing diagram of **2**, viewed along *a*-axis.
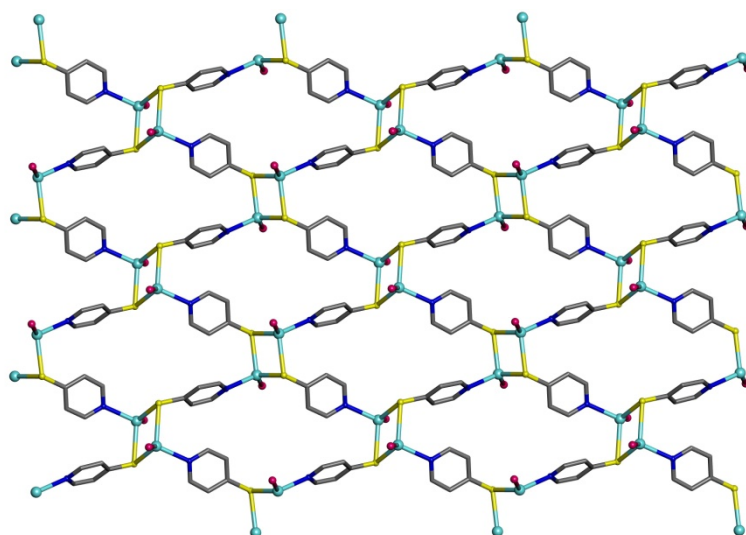
Figure S2: Two dimensional network structure of **3**. The phenyl rings of PPh$_3$ were omitted for clarity. Considering the centroids of the Ag$_2$S$_2$ rings as node, the coordination polymer can be approximated as (4,4) connected network.
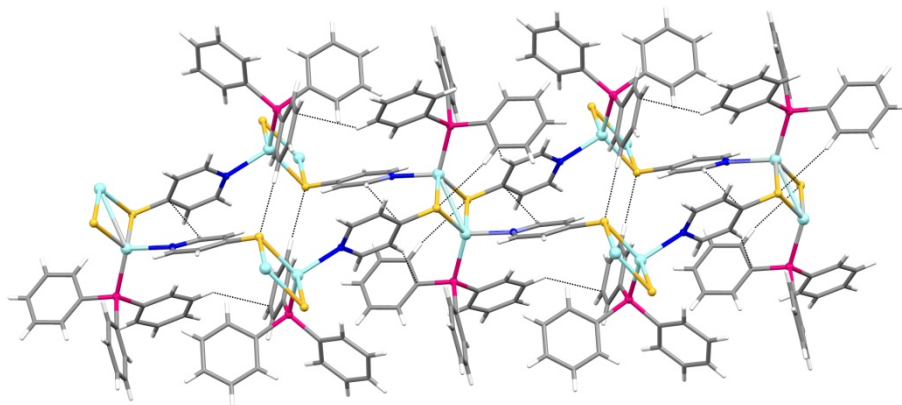
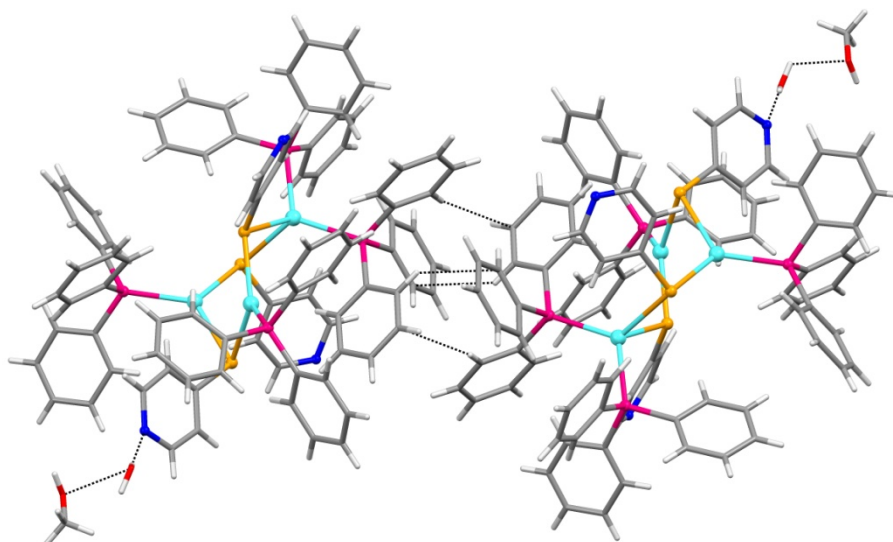Figure S3: The weak C-H$\cdots$S and C-H$\cdots$C(π) interactions in the polymeric network of **3**.

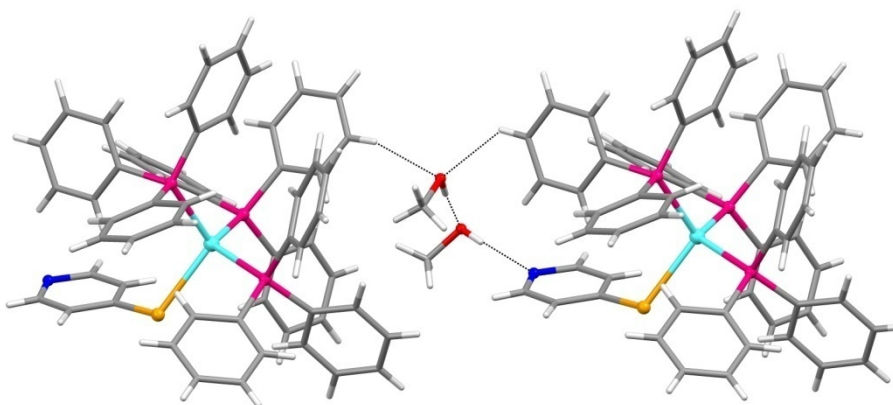Figure S4: Intermolecular interactions in **4**, O-H···N and O-H···O hydrogen bonding and weak C-H···C(π) interactions.

Figure S5: Intermolecular O-H···N, O-H···O and weak C-H···O hydrogen bonding interactions in **5**.
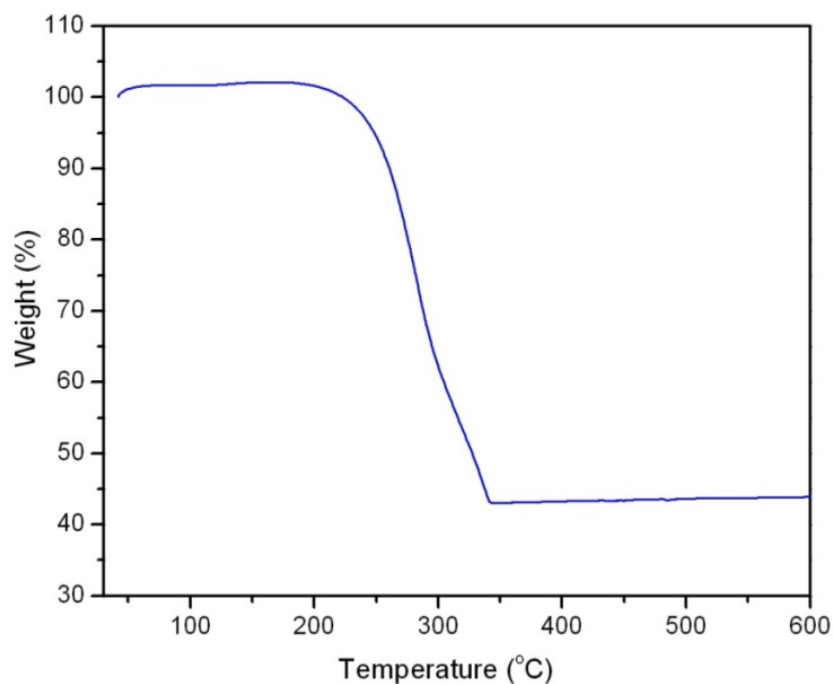
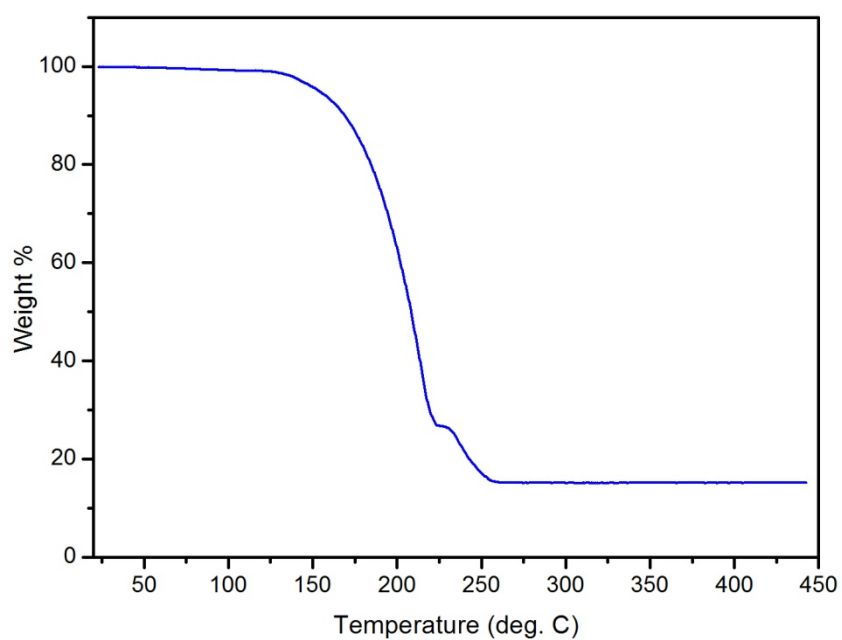Figure S6: TGA plot of **1**. Total weight loss is 58.7%, not matching for the formation of Ag_2S.

Figure S7: TGA plot for **2**. The weight loss occurs in two steps. The first step is for four PPh_3 molecules (observed 72.5 %, calculated 70.5%) and second step is for one pyS and sulfur (observed 11.4% calculated 12.6%). The remaining weight is 16.8% which corresponds to the formation of Ag_2S (calculated value is 16.7%).
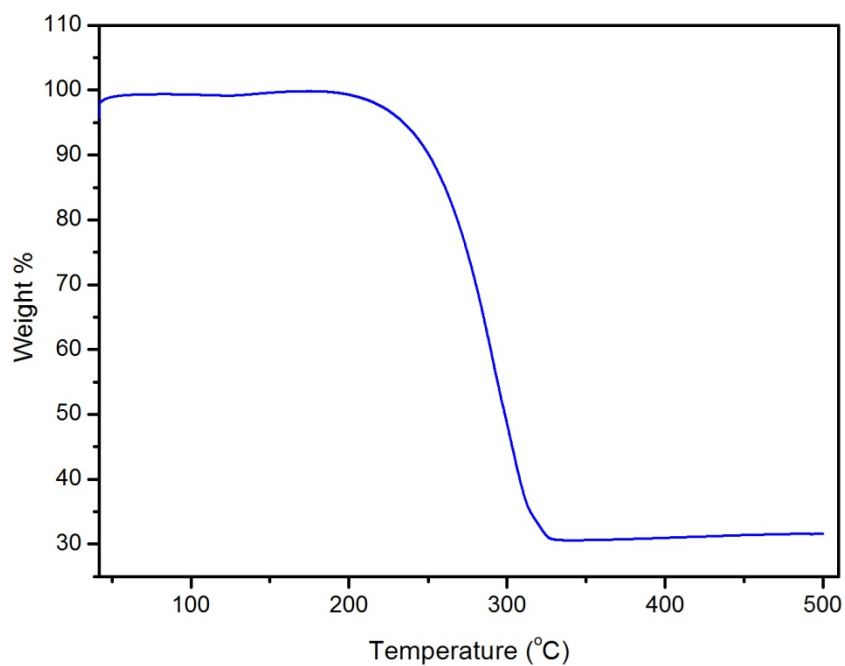
Figure S8: TGA plot for **3**. The weight loss in single step is 69%, which is not exactly matching for the formation of Ag_2S.
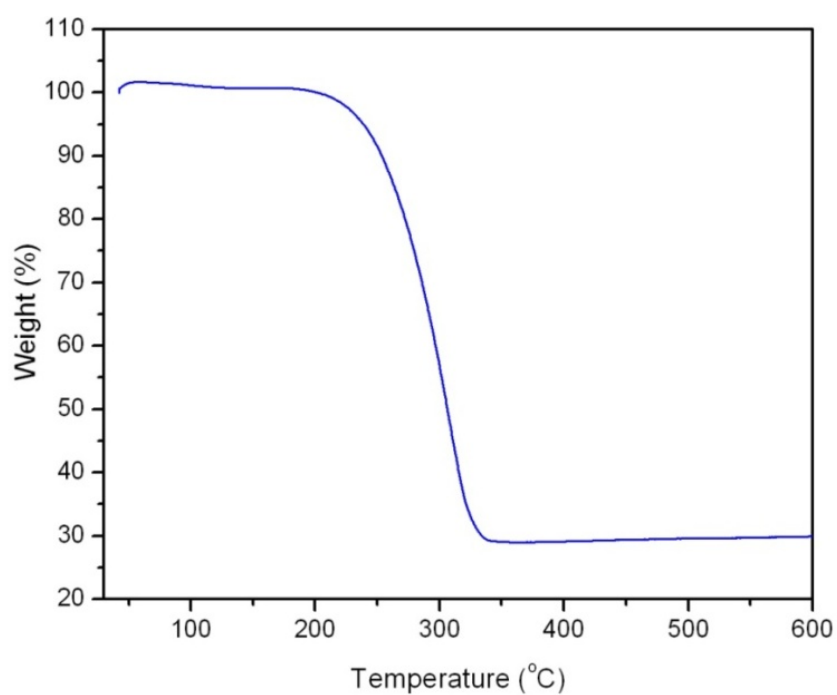

Figure S9: TGA plot for **4**. The residue after decomposition is ~ 28% of the sample used. 24% weight should remain in accordance with Ag_2Se formation.
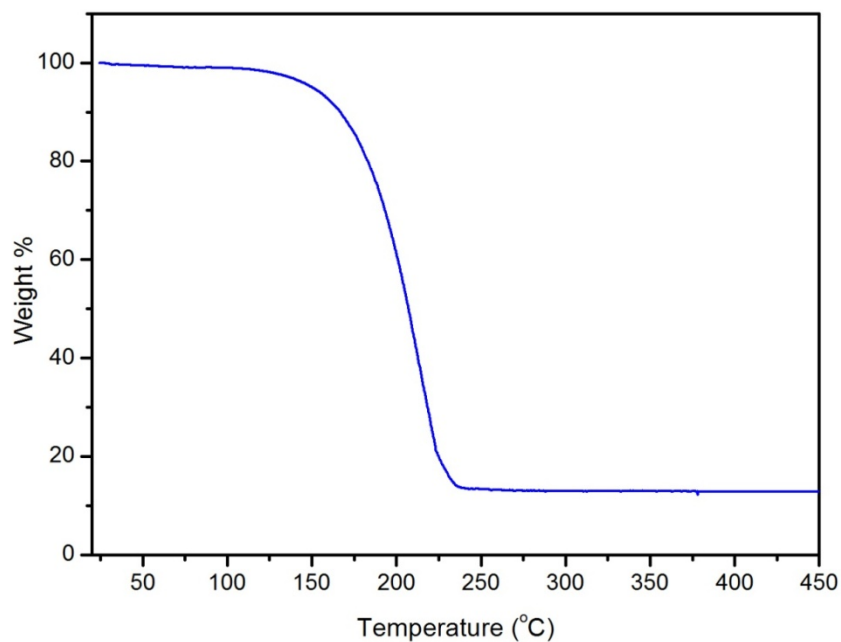
Figure S10: TGA plot for **5**. The weight loss or the decomposition of this complex occurs in single step. The observed weight loss is 86%. The remaining material (14%) corresponds to the formation of Ag_2Se (calculated residue weight 14.0%).
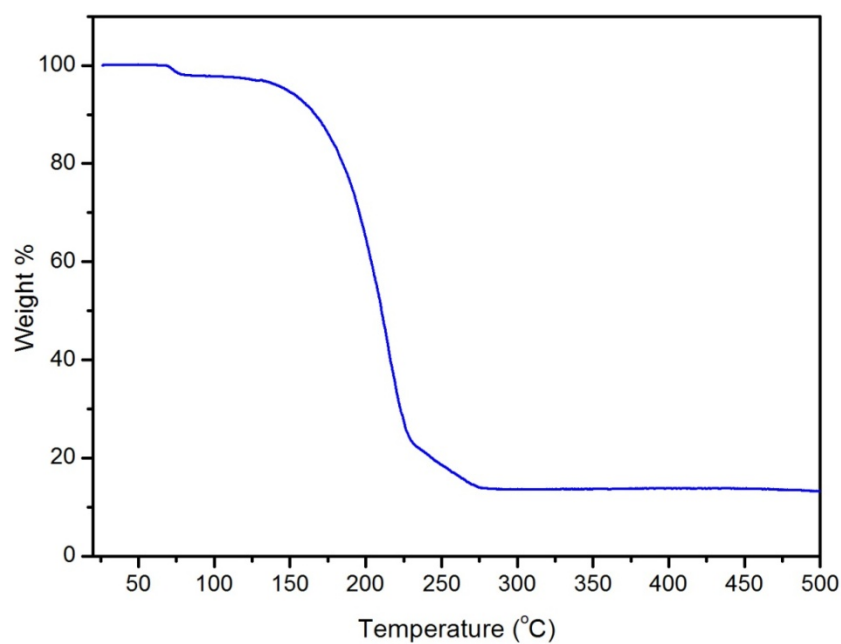

Figure S11: TGA plot for **6·**MeOH. The weight loss of 2.3% observed at 70°C is due to the loss of lattice methanol molecule. The total weight loss is 90.7%. In order to form Ag_2S upon decomposition, the remaining weight should be 12%. The observed remaining weight of 9.3% corresponds to the formation of elemental silver (calculated value 10.4%).
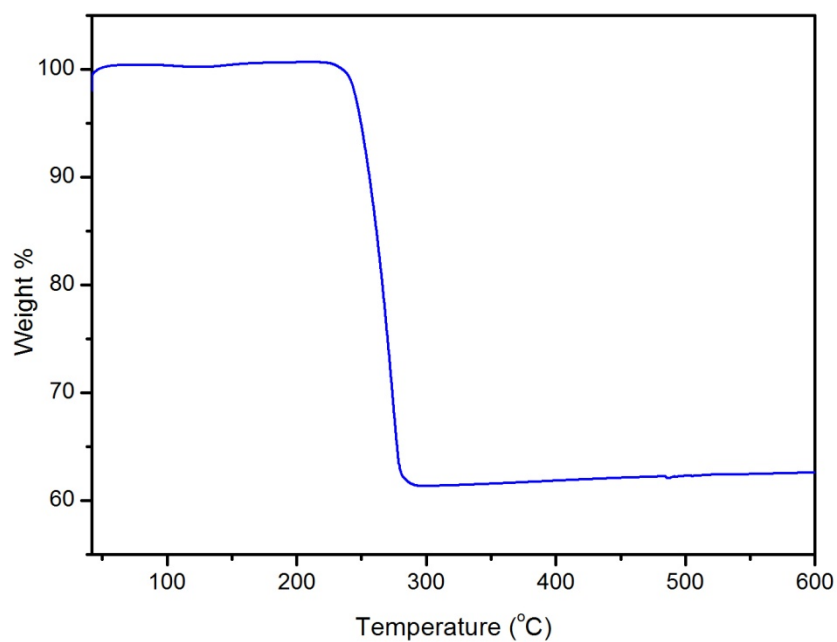
Figure S12: TGA plot for 7**a**. The observed weight loss is 39.1% of the sample used. The calculated weight loss would be 43.1% in accordance with Ag_2S formation.
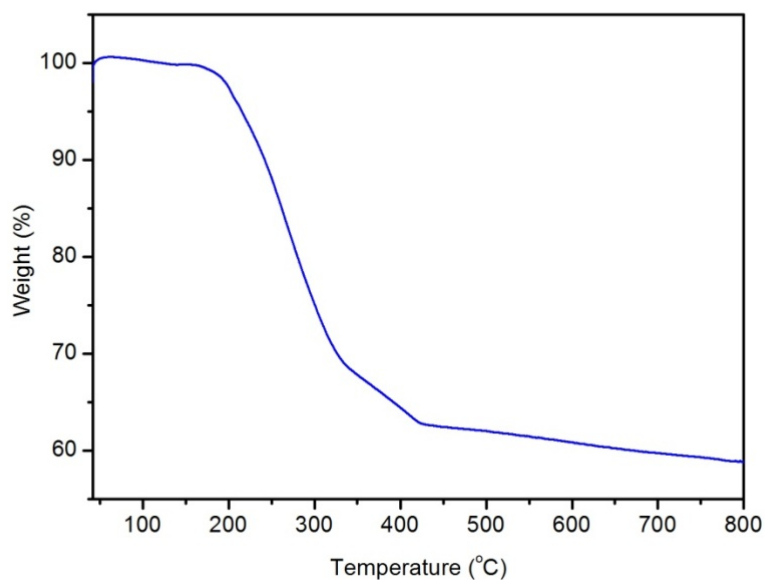

Figure S13: TGA plot for **7b**. Thermal decomposition leads to the formation of Ag_2Se. The residue after decomposition is ~ 59% of the sample used. 55.5% weight should remain in accordance with Ag_2Se formation.
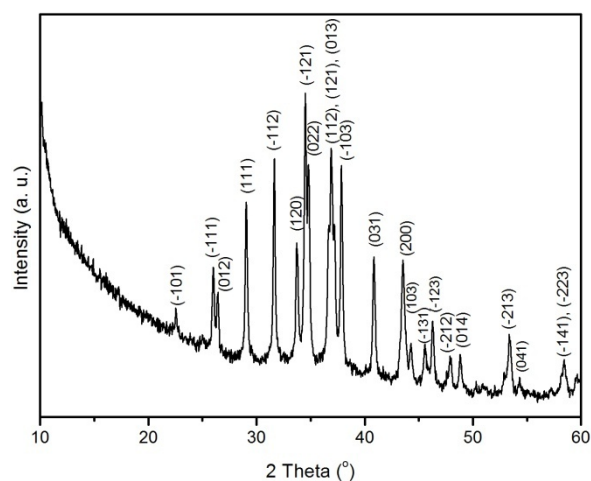
Figure S14: PXRD pattern of Ag$_2$S obtained by thermolysis of **7a** in the solid state
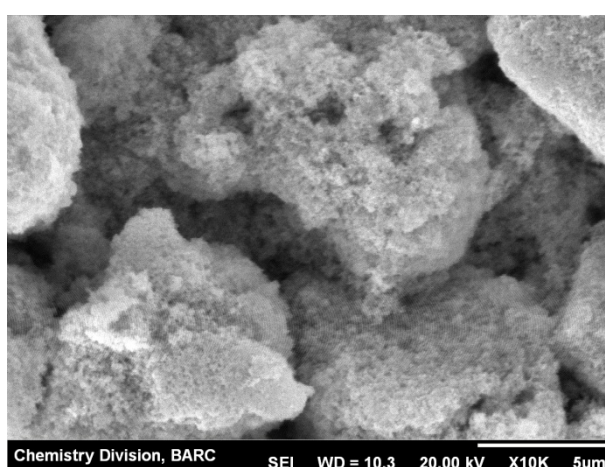

Figure S15: SEM images of Ag$_2$S obtained by solid state pyrolysis of **7a**. The particles are found to be agglomerated. The Ag/S ratio in the EDX analysis was found to be 63.77 / 36.23.
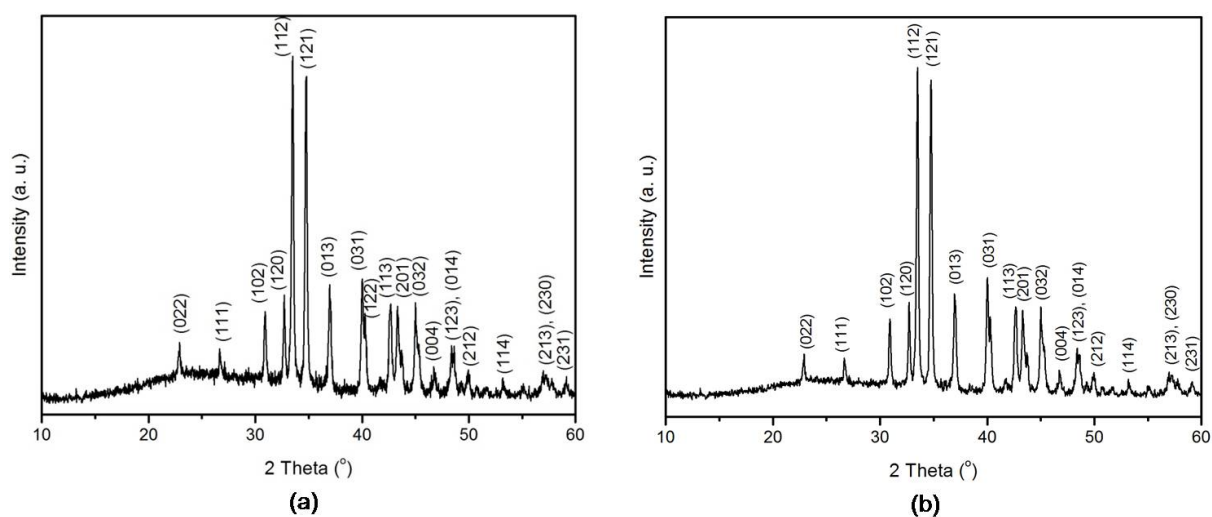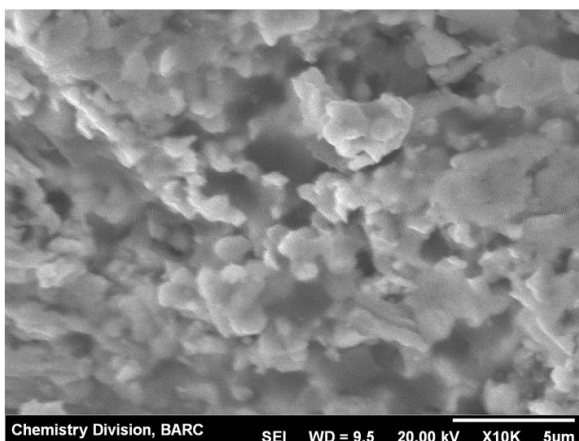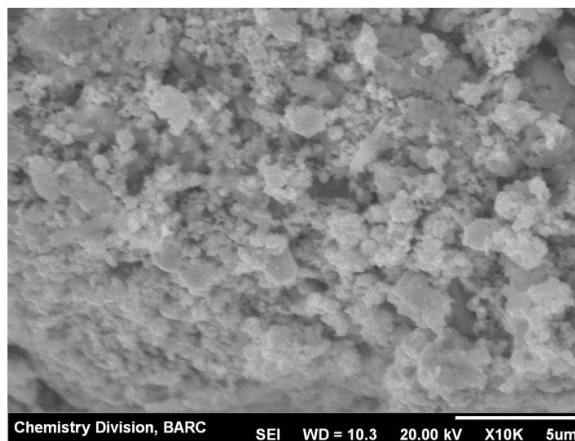

(a)

(b)

Figure S16: The PXRD pattern of the Ag$_2$Se obtained by (a) thermolysis of **4** in HDA at 270 °C and (b) solid state pyrolysis of **5**.

(a)   (b)

Figure S17: SEM images of Ag$_2$Se obtained by (a) thermolysis of **4** in HDA at 270 °C and (b) solid state pyrolysis of **5**. The particles are found to be agglomerated. The Ag / Se ratio in EDX analysis were found to be (a) 66.97 / 33.03 and (b) 69.96 / 33.04.